

Processing of Silica-Bonded Silicon Carbide Ceramics

Yong-Seong Chun and Young-Wook Kim[†]

Department of Materials Science and Engineering, The University of Seoul, Seoul 130-743, Korea

(Received June 9, 2006; Accepted June 19, 2006)

ABSTRACT

The effect of the processing parameters on the sintered density and strength of silica-bonded SiC (SBSC) ceramics was investigated for three types of batches with different particle sizes. The SBSC ceramics were fabricated by an oxidation-bonding process. The process involves the sintering of powder compacts in air so that the SiC particles bond to each other by oxidation-derived SiO₂ glass or cristobalite. A finding of this study was that a higher flexural strength was obtained when the starting powder was smaller. When a ~0.3-μm SiC powder was used as a starting powder, a high strength of 257±42 MPa was achieved at a relative density of ~80%.

Key words: Silicon carbide, Silica-bonded silicon carbide, Processing, Strength

1. Introduction

The combination of the excellent properties of silicon carbide, such as its high hardness, high hot strength, high thermal conductivity, good chemical resistance, and excellent thermal shock resistance, makes ceramics viable for various applications in nozzles, mechanical seals, refractories, bearings, or high-temperature filters.¹⁻⁶⁾ However, high costs due to the high sintering temperature (>2000°C for solid state sintering and >1900°C for liquid-phase sintering) and expensive diamond machining have restricted further uses for ceramics. One approach for producing SiC ceramics at lower temperatures (~1500°C) is the reaction-bonding technique. Reaction-bonded SiC (RBSC) provides an economical advantage due to the lower sintering temperature involved and near absence of dimensional change during fabrication.^{2,3,7,8)}

Recently, an oxidation bonding process was developed for fabricating porous silicon carbide ceramics.^{9,10)} The strategy adopted for making porous SiC ceramics entails the following: fabricating a formed body through a combination of SiC and a pore former, e.g., polymer microbeads or graphite powders followed by sintering the formed body in air. SiC particles are bonded to each other by oxidation-derived SiO₂-glass. The oxidation-bonding technique is also applicable for fabricating SiO₂-bonded SiC ceramics (SBSC). In this paper, the effect of the processing parameters on the sintered density and strength of SBSC is investigated for three types of batches with different particle sizes. In addition, a processing window for fabricating high-strength SBSC is suggested.

2. Experimental Procedure

Three types of SiC powders were used as raw materials. The characteristics of the SiC starting powders and batch compositions are listed in Tables 1 and 2, respectively. All individual batches were mixed in ethanol for 6 h using SiC balls and a polyethylene jar after 2 wt% poly (ethylene glycol) was added as a binder. The mixed slurry was dried and uniaxially pressed into rectangular hexahedrons at 20 MPa. The green compacts were heat-treated at temperatures ranging from 1300°C to 1550°C for 1 h with a heating rate of 2°C/min in air. To investigate the effect of the sintering time, some specimens were sintered at 1350°C for 1-8 h.

The bulk density (D_b) of SBSC was computed from the weight-to-volume ratio. The theoretical density (D_{th}) of SBSC was estimated by the rule of mixtures:

$$D_{th} = (1 - V_{SiO_2}) D_{SiC} + V_{SiO_2} D_{SiO_2} \quad (1)$$

where D_{SiC} and D_{SiO_2} are the theoretical densities of SiC (3.2 g/cm³) and SiO₂ (2.3 g/cm³), respectively, and V_{SiO_2} is the volume fraction of SiO₂ in the specimen. Simply, V_{SiO_2} was calculated from the weight change of the specimen during the heat-treatment in air.¹⁰⁾

The microstructures were observed by Scanning Electron Microscopy (SEM). Using CuKα radiation, X-Ray Diffractometry (XRD) was performed on ground powders. For the flexural strength measurements, bar-shaped samples were machined to a size of 3×4×35 mm. Bend tests were performed at room temperature using a four-point method with an inner and outer span of 10 and 20 mm, respectively. A total of 81 specimens were measured using a crosshead speed of 0.5 mm/min.

[†]Corresponding author: Young-Wook Kim
E-mail: ywkim@uos.ac.kr
Tel: +82-2-2210-2760 Fax: +82-2-2215-5863

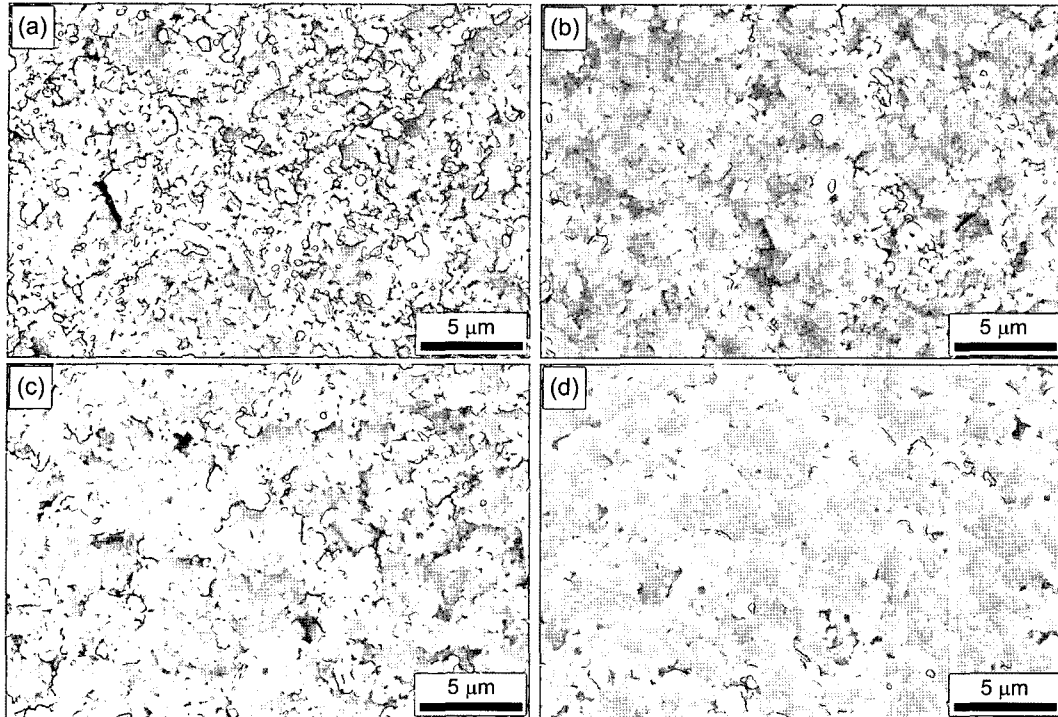


Fig. 1. Typical fracture surfaces of silica-bonded SiC ceramics (SBSC1) sintered at various temperatures for 1 h in air; (a) 1300°C, (b) 1350°C, (c) 1400°C, and (d) 1550°C.

Table 1. SiC Powder Characteristics and Designation

Characteristic	Type of powder		
Designation	SiC 1 (Ultrafine)	SiC 2 (FCP15C)	SiC 3 (#220)
Average particle size (μm)	0.32	0.50	65.0
Specific surface area (m^2/g)	20.0	15	—
Crystalline phase	β	α	α
Impurity (wt%)			
Oxygen	0.22	0.40	0.29
Free carbon	0.87	0.20	0.04
Manufacturer	Ibiden Co., Ltd., Ogaki, Japan	Norton As, Eydehavn, Norway	Showa Denko, Tokyo, Japan

3. Results and Discussion

Typical fracture surfaces of several selected SBSC1 ceramics are shown in Fig. 1. As shown, moderately dense microstructures were achieved. A submicron grain size was maintained up to 1350°C, while a small amount of grain growth was observed at higher temperatures. The observed pore sizes were mostly less than 1 micrometer in all specimens, and the pores were distributed homogeneously.

Table 2. Batch Composition of Silica-Bonded SiC Ceramics (wt%)

Sample designation	SiC 1	SiC 2	SiC 3
SBSC1	100	—	—
SBSC2	—	100	—
SBSC3	—	30	70

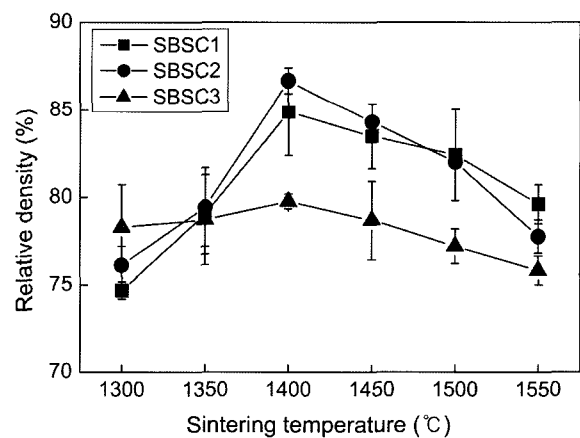
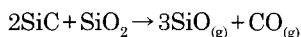


Fig. 2. Relative density of silica-bonded SiC ceramics as a function of sintering temperature. All samples were sintered for 1 h in air (refer to Table 2).

Fig. 2 shows variations in relative density as a function of sintering temperature. As shown, the relative density increased as the sintering temperature increased from 1300°C to 1400°C for all specimens. However, a further increase in temperature to above 1400°C decreased the relative density. The heating of the SiC powder compacts to temperatures ranging from 1300°C to 1550°C followed by isothermal holding within that range of temperatures in air allowed for the oxidation of the SiC powders. This formed oxidation-derived silica as a bonding phase between SiC particles, and resulted in SBSC.^{9,10} It is expected that the amount of oxidation-derived silica increases as the sintering time increases. In SBSC3, the change in sintering temperature does not noticeably affect the sintered density due to the large SiC grit (~65 μm) in the starting powder. The oxidation rate of the large SiC grit should be especially slow, compared to those of the submicron SiC powders. The oxidation-derived SiO₂ contents in SBSC1 and SBSC3, which were sintered at 1350°C for 1 h, were 25.6% and 12.5%, respectively.

Phase analysis by XRD (Fig. 3) showed the presence of only β-SiC as a crystalline phase up to 1450°C, indicating the formation of amorphous SiO₂ as an oxidation product of SiC. However, sintering at 1500°C led to the crystallization of the amorphous SiO₂ into cristobalite.

Densification of SBSC may start between 800-1000°C, and probably follows a similar mechanism as that which was proposed for the sintering of amorphous SiO₂ by a viscous sintering process.¹¹ The decrease in the density above 1400°C was due to the reaction between SiC and SiO₂ that involves volatilization of SiO and CO gases, as in the following reaction:¹²



Essentially, specimens sintered at 1550°C showed many bubbles on the surface caused by the entrapment of the reaction product gases. Thus, the strength of the specimens sintered at 1550°C could not be measured. Fig. 1(d) showed a denser microstructure compared to others, as the above reac-

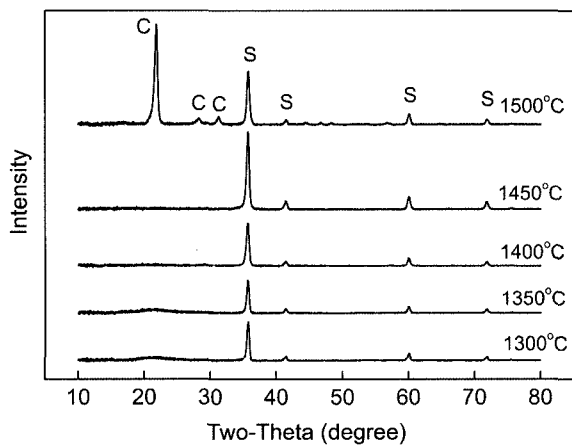


Fig. 3. XRD patterns of SBSC1 samples sintered at various temperatures for 1 h in air (C and S denote cristobalite and β-SiC, respectively).

tion took place preferentially on the surface of the specimen.

Typical fracture surfaces of SBSC2 and SBSC3 sintered at 1350°C for 1 h are shown in Fig. 4. The grain sizes of the specimens were larger compared to the grain size of SBSC1, which was sintered at the same temperature (see Fig. 1(b)), indicating minimal grain growth at 1350°C. Large SiC grits that bonded with oxidation-derived SiO₂ are shown in Fig. 4(b). Thus, the comparably large starting powder led to a larger grain size in this process.

The effect of the sintering time on the sintered density at 1350°C is shown in Fig. 5. The densities of SBSC1 and

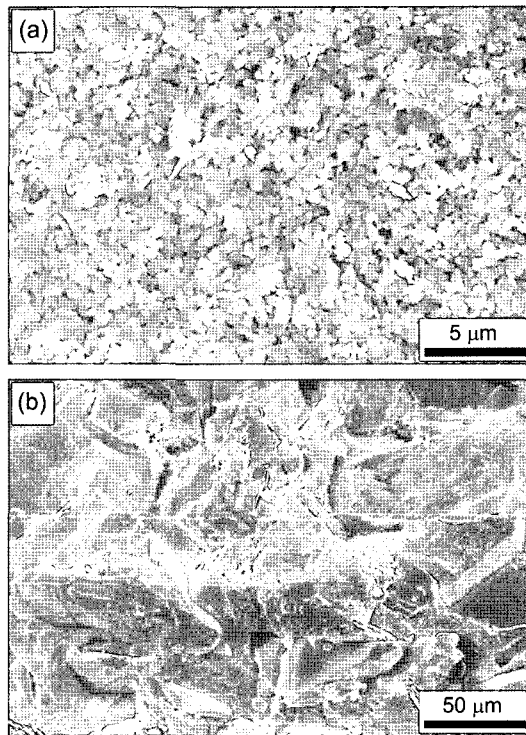


Fig. 4. Typical fracture surfaces of silica-bonded SiC ceramics sintered at 1350°C for 1 h in air; (a) SBSC2 and (b) SBSC3.

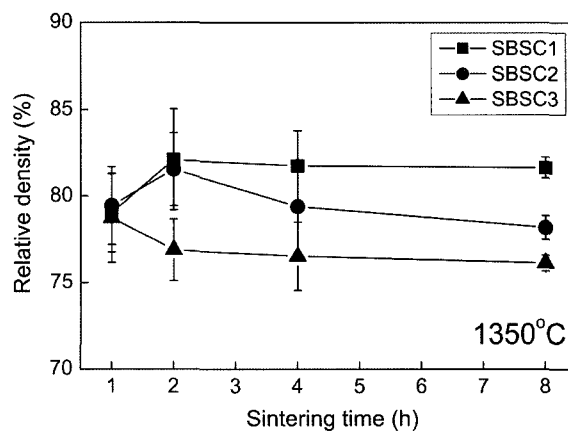


Fig. 5. Relative density of silica-bonded SiC ceramics as a function of sintering time at 1350°C in air (refer to Table 2).

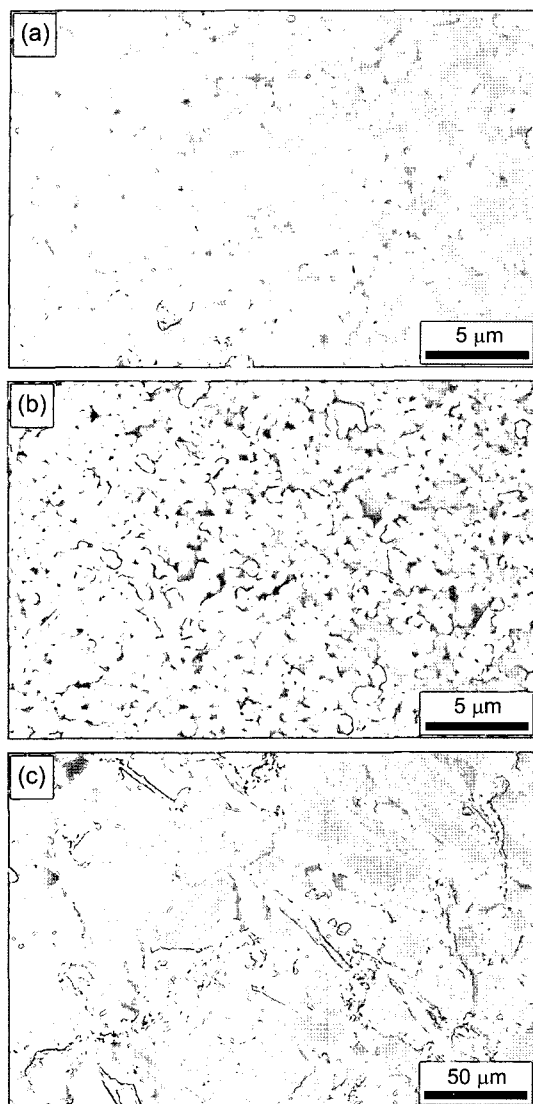


Fig. 6. Typical fracture surfaces of silica-bonded SiC ceramics sintered at 1350°C for 8 h in air; (a) SBSC1, (b) SBSC2, and (c) SBSC3.

SBSC2 increased slightly after sintering for 2 h while that of SBSC3 decreased slightly after sintering for 2 h. Further elongation of the sintering time led to no density change in either SBSC1 or SBSC3. Typical fracture surfaces of specimens sintered for 8 h are shown in Fig. 6. Compared to the specimen sintered for 1 h, a near absence of grain growth was observed in these specimens, indicating that the viscosity of the oxidation-derived silica was fairly high at 1350°C. However, an XRD analysis on the 8-h sintered specimens showed the presence of cristobalite (see Fig. 7), indicating that the oxidation of SiC and the crystallization of oxidation-derived silica proceed simultaneous at 1350°C. The absence of the cristobalite peaks in SBSC1 after 1-h sintering at 1350°C (see Fig. 3) was due to the short-oxidation time. Thus, the cristobalite phase was crystallized at 1500°C after 1 h of sintering and at 1350°C after 8 h of sintering. Accordingly, the bonding phase between SiC grains

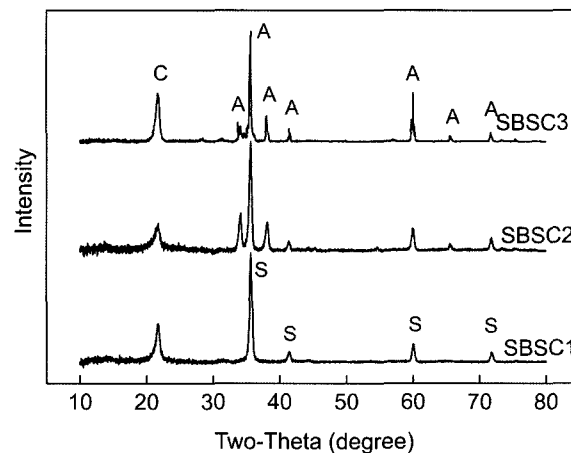


Fig. 7. XRD patterns of silica-bonded SiC ceramics sintered at 1350°C for 8 h in air (C, A, and S denote cristobalite, α -SiC, and β -SiC, respectively).

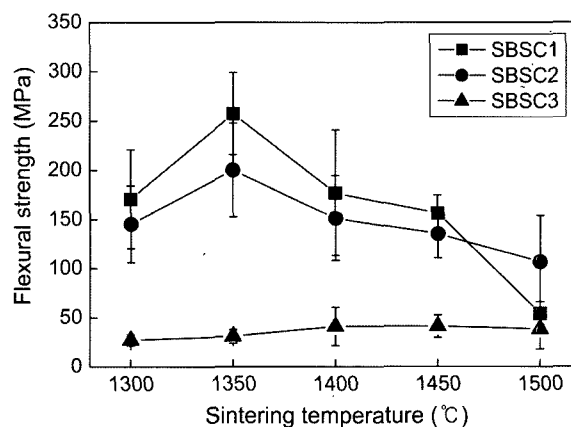


Fig. 8. Flexural strength of silica-bonded SiC ceramics as a function of sintering temperature. All samples were sintered for 1 h in air (refer to Table 2).

in SBSC appears to be identical for specimens sintered at a low temperature for longer periods and for specimens sintered at a high temperature for shorter periods. The α -SiC peaks observed in SBSC2 and SBSC3 (Fig. 7) are originated from the starting powders (see Table 1).

Fig. 8 illustrates the flexural strength as a function of sintering time for the samples sintered for 1 h. The flexural strength was strongly affected by the starting particle size. The smaller the starting powder, the higher the flexural strength obtained. The flexural strength was the highest at 1350°C for both SBSC1 and SBSC2; whereas for SBSC3, nearly no change in the strength was observed. It is interesting that the sintered density showed a maxima at a sintering temperature of 1400°C (see Fig. 2), while the flexural strength showed a maxima at a sintering temperature of 1350°C. The relative densities of the SBSC1 specimens sintered at 1350°C and 1400°C for 1 h were 79.0% and 84.9%, respectively. In contrast, the strengths of the SBSC1 specimens sintered at 1350°C and 1400°C for 1 h were 257 ± 42

MPa and 177 ± 64 MPa, respectively. The relative densities of the SBSC2 specimens sintered at 1350°C and 1400°C for 1 h were 79.4% and 86.7%, respectively. In contrast, the strengths of the SBSC2 specimens sintered at 1350°C and 1400°C for 1 h were 200 ± 48 MPa and 151 ± 43 MPa, respectively. The highest density ($\sim 86\%$) was obtained at 1400°C , but the best strength (257 ± 42 MPa) was obtained at 1350°C . Generally, the flexural strength of porous ceramics decreases as the porosity increases.¹³⁻¹⁵ A 5% increase in the sintered density leads to a significant increase in strength; however, a contradictory tendency was observed in SBSC1 and SBSC2. This discrepancy is attributed to the contribution of residual stresses while determining the strength. This indicates that the residual stresses that develop by the thermal expansion mismatch between the SiC and oxidation product (silica or cristobalite depending on sintering conditions) should be involved in the measured strength of specimens. The crystallization of oxidation-derived silica into cristobalite leads to a degradation of strength (see Figs. 8 and 9). It is evident that sintering at 1350°C for 1 h leads to the optimum residual stresses for the strengthening of SBSC. Additionally, the higher strength of SBSC1 and SBSC2 relative to SBSC3 may be correlated with both the weak bonding between SiC grits and the presence of large pores in SBSC3. A comparison of the fracture surfaces of SBSC1 (Fig. 1(b)) with SBSC2 (Fig. 4(a)) shows that SBSC1 has a notably smaller grain size and a smaller pore size. This may lead to a relatively higher strength for SBSC1 in comparison with SBSC2, as the mechanical strength of porous ceramics generally decreases as the pore size increases.^{15,16} Thus, a smaller starting powder leads to a higher strength in this process.

The effect of the sintering time on the flexural strength is shown in Fig. 9. As shown, both SBSC1 and SBSC2 show some degradation in strength when the sintering time is longer than 1 h. This result also supports the above suggestion. The strength variation of SBSC3 with sintering temperature and sintering time was especially small due to the

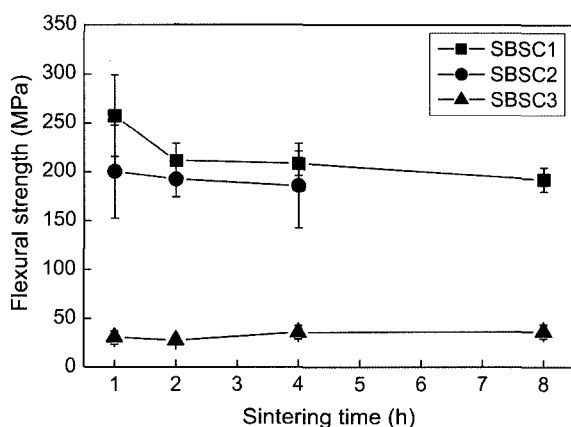


Fig. 9. Flexural strength of silica-bonded SiC ceramics as a function of sintering time at 1350°C in air (refer to Table 2).

presence of large SiC grit ($\sim 65 \mu\text{m}$) particles in the starting compacts. Compared to the submicron SiC powders, the oxidation rate of large SiC grit is relatively slow, leading to weaker bonding between each grain.

4. Conclusions

High strength silica-bonded SiC ceramics were fabricated at a temperature as low as 1350°C . It was shown that the strength of silica-bonded SiC ceramics is strongly dependent on the initial particle size. At a given processing condition, smaller particles resulted in a higher strength. For submicron powders, a combination of sintering temperature of 1350°C and a sintering time of 1 h resulted in the best strength. For the samples prepared from $\sim 0.3\text{-}\mu\text{m}$ particles, a high strength of 257 ± 42 MPa was achieved at a relative density of $\sim 80\%$.

REFERENCES

- G. D. Zhan, M. Mitomo, R. J. Xie, and A. K. Mukherjee, "Thermal and Electrical Properties in Plasma-Activation-Sintered Silicon Carbide with Rare-Earth-Oxide Additives," *J. Am. Ceram. Soc.*, **84** [10] 2448-50 (2001).
- I. S. Han, K. S. Lee, D. W. Seo, and S. K. Woo, "Improvement of Mechanical Properties in RBSC by Boron Carbide Addition," *J. Mater. Sci.*, **21** 703-06 (2002).
- S. S. Hwang and T. W. Kim, "Fabrication and Properties of Reaction Bonded SiC Hot Gas Filter Using Si Melt Infiltration Method (in Korean)," *J. Kor. Ceram. Soc.*, **40** [9] 891-96 (2003).
- S. H. Lee and Y.-W. Kim, "Effect of Additive Composition on Mechanical Properties of Silicon Carbide Sintered with Aluminum Nitride and Erbium Oxide," *J. Kor. Ceram. Soc.*, **42** [1] 16-21 (2005).
- Y. S. Chun and Y.-W. Kim, "Possible Strategies for Microstructure Control of Liquid-Phase-Sintered Silicon Carbide Ceramics," *J. Kor. Ceram. Soc.*, **42** [8] 542-47 (2005).
- Y.-W. Kim, S. H. Lee, T. Nishimura, and M. Mitomo, "Heat-Resistant Silicon Carbide with Aluminum Nitride and Scandium Oxide," *Acta Mater.*, **53** 4701-08 (2005).
- S. S. Hwang, S. W. Park, J. H. Han, K. S. Han, and C. M. Kim, "Mechanical Properties of Porous Reaction Bonded Silicon Carbide (in Korean)," *J. Kor. Ceram. Soc.*, **39** [10] 948-54 (2002).
- H. W. Jun, H. W. Lee, H. Song, B. H. Kim, and J. Ha, "Reaction-Bonded Silicon Carbide Tube Fabricated by Continuous Sintering of Double-Walled Preform," *Ceram. Int.*, **30** 533-37 (2004).
- J. H. She, T. Ohji, and S. Kanzaki, "Oxidation Bonding of Porous Silicon Carbide Ceramics with Synergistic Performance," *J. Eur. Ceram. Soc.*, **24** 331-34 (2004).
- Y. S. Chun and Y.-W. Kim, "Processing and Mechanical Properties of Porous Silica-Bonded Silicon Carbide Ceramics," *Metal Mater. Int.*, **11** [5] 351-55 (2005).
- V. Yaroshenko and D. S. Wilkinson, "Sintering and Microstructure Modification of Mullite/Zirconia Composites Derived from Silica-Coated Alumina Powders," *J. Am.*

- Ceram. Soc.*, **84** [4] 850-58 (2001).
12. Y.-W. Kim, H. Tanaka, M. Mitomo, and S. Otani, "Influence of Powder Characteristics on Liquid Phase Sintering of Silicon Carbide," *J. Ceram. Soc. Jpn.*, **103** [3] 257-61 (1995).
 13. S. H. Kim, Y.-W. Kim, J. Y. Yun, and H. D. Kim, "Fabrication of Porous SiC Ceramics by Partial Sintering and their Properties(in Korean)," *J. Kor. Ceram. Soc.*, **41** [7] 541-47 (2004).
 14. Y.-W. Kim, H. D. Kim, and C. B. Park, "Processing of Microcellular Mullite," *J. Am. Ceram. Soc.*, **88** [12] 3311-15 (2005).
 15. Y.-W. Kim, Y. J. Jin, Y. S. Chun, I. H. Song, and H. D. Kim, "A Simple Processing Route to Closed-Cell Microcellular Ceramics," *Scripta Mater.*, **53** 921-25 (2005).
 16. D. M. Liu, "Influence of Porosity and Pore Size on the Compressive Strength of Porous Hydroxyapatite Ceramic," *Ceram. Int.*, **23** 135-39 (1997).